



Measurements of light-absorbing particles on the glaciers in the Cordillera Blanca, Peru

C. G. Schmitt^{1,2}, J. D. All^{3,2}, J. P. Schwarz^{4,5}, W. P. Arnott⁶, R. J. Cole^{7,2,*}, E. Lapham², and A. Celestian³

¹National Center for Atmospheric Research, Boulder, Colorado, USA

²American Climber Science Program, Eldora, Colorado, USA

³Department of Geography and Geology, Western Kentucky University, Bowling Green, Kentucky, USA

⁴Chemical Sciences Division, Earth System Research Laboratory, National Oceanic and Atmospheric Administration, Boulder, Colorado, USA

⁵Cooperative Institute for Research in Environmental Sciences, University of Colorado, Boulder, Colorado, USA

⁶Department of Physics, University of Nevada, Reno, Nevada, USA

⁷Institute of Arctic and Alpine Research, University of Colorado, Boulder, Colorado, USA

* now at: Department of Natural Resources and Environmental Management, University of Hawaii, Manoa, Hawaii, USA

Correspondence to: C. G. Schmitt (schmittc@ucar.edu)

Received: 28 July 2014 – Published in The Cryosphere Discuss.: 8 October 2014

Revised: 10 January 2015 – Accepted: 15 January 2015 – Published: 12 February 2015

Abstract. Glaciers in the tropical Andes have been rapidly losing mass since the 1970s. In addition to the documented increase in temperature, increases in light-absorbing particles deposited on glaciers could be contributing to the observed glacier loss. Here we report on measurements of light-absorbing particles sampled from glaciers during three surveys in the Cordillera Blanca Mountains in Peru. During three research expeditions in the dry seasons (May–August) of 2011, 2012 and 2013, 240 snow samples were collected from 15 mountain peaks over altitudes ranging from 4800 to nearly 6800 m. Several mountains were sampled each of the 3 years and some mountains were sampled multiple times during the same year. Collected snow samples were melted and filtered in the field then later analyzed using the Light Absorption Heating Method (LAHM), a new technique that measures the ability of particles on filters to absorb visible light. LAHM results have been calibrated using filters with known amounts of fullerene soot, a common industrial surrogate for black carbon (BC). As sample filters often contain dust in addition to BC, results are presented in terms of effective black carbon (eBC). During the 2013 survey, snow samples were collected and kept frozen for analysis with a Single Particle Soot Photometer (SP2). Calculated eBC mass from the LAHM analysis and the SP2 refractory black carbon (rBC) results were well correlated ($r^2 = 0.92$). These re-

sults indicate that a substantial portion of the light-absorbing particles in the more polluted regions were likely BC. The 3 years of data show that glaciers in the Cordillera Blanca Mountains close to human population centers have substantially higher levels of eBC (as high as 70 ng g^{-1}) than remote glaciers (as low as 2.0 ng g^{-1} eBC), indicating that population centers can influence local glaciers by sourcing BC.

1 Introduction

A substantial portion of the population of South America lives on the west coast, where the water supply is supported by the runoff from glacier melt (Barnett et al., 2005). When a region with glaciers is experiencing warming, the water availability for the region will change even if precipitation patterns remain constant. Initially, runoff from glaciers will increase as melting increases, but eventually the glacier area will be sufficiently reduced so that the increased melting rate will be offset by the decreased glacier area available for melting and increased water loss due to evaporation, sublimation, or absorption into ground surfaces. Thus, over time the typical water discharge increases as warming starts, reaches a peak, then reduces until a new steady state is reached, presumably after the climate has stopped changing or after the

glaciers have completely melted (Baraer et al., 2012). Post warming water flow rates are expected to be significantly below pre-warming flow rates. If glacier melt becomes insignificant, surface water flow rates are then driven more by precipitation, and as a result, dry season water flows can be substantially reduced while wet season flows may not be as significantly impacted. Baraer et al. (2012) estimated the evolution of water flow rates for the Cordillera Blanca region. Their results show that most valleys are past their highest levels of runoff, implying diminishing water supplies into the future if melting persists. The effect of increased BC and dust on this glacial “life cycle” is to accelerate the process. Increased BC and dust will lead to faster glacier recession, though it is unclear what the effect on runoff would be during the transition phase.

In our warming climate, glaciers are melting at a fast rate and tropical glaciers are being substantially impacted. Glaciers in Peru account for more than 70 % of the world’s tropical glacial area (Kaser, 1999). Rabatel et al. (2013) showed that glaciers in the tropical Andes have receded in area approximately 30 % since the 1970s and that areal loss rates have increased substantially in the first decade of the new millennium. Vuille et al. (2008) showed that surface air temperature has increased by 0.10 °C per decade over the last 70 years in the tropical Andes based on measurements from 279 stations between 1° N and 23° S. Similar trends have been shown to exist in studies focusing on temperature evolution in the last several decades from National Centers for Environmental Prediction/National Center for Atmospheric Research (NCEP/NCAR) climate reanalysis data (Kalnay et al., 1996; Bradley et al., 2009). Mark and Seltzer (2003) used NCEP/NCAR reanalysis data to show that the freezing elevation in the Cordillera Blanca, the location of this study, has risen approximately 200 m between 1955 and 2003. Using climate models, Bradley et al. (2006) have shown that tropical glacial regions (above 5000 m) could experience 4 to 5 °C of temperature increase between 2000 and 2100.

In addition to air temperature changes, dust and BC deposited on snow could potentially be a major factor leading to glacial mass loss. BC and dust reduce snow’s albedo by absorbing solar radiation, which leads to increased melt and sublimation rates (Warren and Wiscombe, 1980). It has recently been shown by Painter et al. (2013) that BC likely led to the end of the little ice age in the European Alps in the mid-1800s. Dust on snow in Colorado has led to substantially increased melt rates (Painter et al., 2012) and has decreased total runoff (Painter et al., 2010). The effects of BC on snow in the Northern Hemisphere has been subject to intensive study, however, despite the fact that glaciers are a critical water source for large populations in South America, no studies to date have measured BC and dust in this region.

The Cordillera Blanca range is located in north central Peru. The mountain range is home to 17 peaks over 6000 m and hundreds over 5000 m. The bulk of precipitation comes from the Amazon basin in the wet season, which gener-

ally runs from October until May. During the dry season, the atmospheric flows generally come from the west and include more dry air. The dry season in the Cordillera Blanca is not completely dry as it is possible for small storms to pass through the range typically on a weekly basis. These dry season storms can produce snow from a few centimeters to a few tens of centimeters which can sometimes obscure the expected variability of light-absorbing particles by depth. Schauwecker et al. (2014) estimated that for the Cordillera Blanca region, there has been a modest temperature increase as well as a modest (60 mm decade⁻¹) increase in precipitation since the early 1980s. They state that recent changes in temperature and precipitation alone may not explain the glacial recession observed in the 30 years ending in 2012.

Sources of BC and dust in the Cordillera Blanca are numerous. Obvious anthropogenic sources of BC include industry and transportation (especially from diesel-fueled vehicles). Industrial sources are mostly centered in and around Huaraz, the largest city (population: 100 000, altitude: 3052 m altitude) abutting the Cordillera Blanca. Regional emission inventories for BC are not available, and emission inventories developed for global models are generally based on national emission statistics and do not contain regional specifics. There is substantial agriculture and BC from agricultural burning in the Cordillera Blanca region. Dust from land clearing and livestock grazing could impact the Cordillera Blanca cryosphere as well. Another potential source of BC is forest clearing and biomass burning in the Amazon basin. Amazonian burning has been estimated to account for approximately 50 % of the carbonaceous aerosols in the Amazon region (Lamarque et al., 2010; Kaiser et al., 2012). Hydroelectric power is one of the most common forms of energy production, and coal burning is not significant in South America. Increases in dust can be caused by agriculture, construction, mining, and increased traffic on dirt roads.

The measurements described in this publication were collected by scientists and volunteers participating in American Climber Science Program (ACSP) expeditions (www.climberscience.com). The ACSP is a research organization with the goal of facilitating research and educational opportunities for scientists and students in regions that are challenging to access. To achieve these goals, experienced climbers are often included in research expeditions in order to increase safety in the mountains. The ACSP research expeditions are also designed to provide opportunities for non-scientists to learn about scientific practices as well as to instruct future scientists on safety in mountain regions. More than 50 international and Peruvian scientists, students, teachers and volunteers have participated in the three ACSP Peru expeditions.

Here, we report on 3 years of measurements of light-absorbing particles sampled on glaciers in the Cordillera Blanca. Section 2 describes the field campaigns and the sample collection methods. Section 3 describes a newly devel-

oped technique for the quantification of light-absorbing particles collected on filters. Section 4 presents the results from the 3 years of measurements, and the final section discusses the main conclusions of the project.

2 Field measurements

The ACSP has conducted three research expeditions during the dry season (austral winter) to the Cordillera Blanca region of Peru beginning in 2011. The sampling of snow and ice for light-absorbing particles has been a primary research project during the three expeditions. During the 3 expeditions, 48, 100, and 90 samples were collected respectively. Samples were taken from glacial surfaces from a minimum altitude of 4800 m and then at regular altitude intervals to the mountain top. Several mountains were sampled during all three expeditions, and some mountains have been sampled more than once during a single expedition. On one occasion multiple samples were taken at different depths by collecting ice from the walls of a crevasse; these data are used to identify long-term trends in particle loadings.

When working in remote and demanding conditions it is important to use simple techniques that provide robust scientific results. Several techniques for snow particle sampling were considered before a filtering technique was chosen. The technique for sampling particles in snow is similar to the technique used by the University of Washington's "Soot in Arctic Snow" group (as described in Doherty et al., 2010).

During research expeditions, volunteer scientists collect snow samples from predetermined locations on each mountain. Samples are collected from approximately 100 m above the snow line to the summit at 200 to 500 vertical meter intervals, the exact interval depends on the height of the mountain and the complexity of the terrain. Volunteers are instructed to avoid areas near exposed rock as well as areas that may be near avalanche paths or could be affected by debris from avalanches. Because mountain climbing is a physically demanding and potentially dangerous activity, the ultimate decisions on how high and where to collect samples is left to the discretion of the climbing team with safety being the highest priority. Global Positioning System waypoints are taken and, if possible, samples are collected from the same location as on previous climbs. Snow samples were collected by scooping snow into 4-liter ziplock plastic bags. Bags are labeled on the outside with a permanent marker after the bag has been sealed. Typically, ACSP volunteers collected samples with hands that had been "contaminated" with local snow. This is done by washing hands with snow so that any contaminants on the hands are similar to those in the snow. Since snow is collected on the descent usually well after sunrise, the snow is soft enough that it is easy to fill a bag contacting the snow only minimally. For each sample approximately 1 kg of snow is collected at each site from both the surface (defined as the top 2.5 cm) and the subsurface (deeper than 2.5 cm). The idea

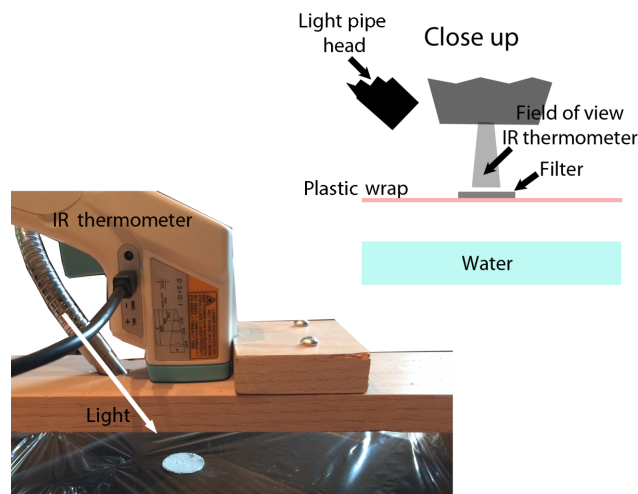


Figure 1. Diagram of the LAHM analysis setup. A light source is aimed at a 45° angle at the filter which rests on plastic wrap approximately 10 cm above the water surface. The infrared thermometer directly views the center of the filter. The field of view of the thermometer is approximately 1.5 cm at the distance of the filter and the contaminant spot on the filter is generally 2 cm in diameter.

was that the surface sample should give an indication of any dry deposition that has occurred since the last snow storm as well as any accumulation of contaminants on the surface due to melting and sublimation while the subsurface samples should contain any contaminants that came with the most recent snowstorm either as ice nuclei or as having been scavenged by falling snow. In reality, it was commonly found that fresh snowfall during the dry season amounted to less than 10 cm. The result was that the subsurface sample often contained snow that had been subject to dry deposition and surface accumulation before the most recent snowfall. Once samples were collected and labeled, the snow samples are packed together into backpacks and returned to base camp for processing.

In camp, snow samples are melted one at a time by placing the ziplock bags in warm water (usually around 30 °C). Once melted, snow-sourced water is drawn into 60 mL syringes and pumped slowly through 0.7 micron "Pallflex Tis-suquartz" type 25 mm quartz fiber filters. A total of 600 mL of snow-water is filtered per sample unless the filter becomes too clogged, in which case less water is filtered, and the amount of filtered water is recorded. The samples are filtered immediately after melting to minimize adhesion of particles to the surface of the bag. The typical time between the starting of melting and the completion of filtering is 15 to 20 min. Filters are removed from filter holders, placed into plastic capsules designed for coin collections, and held in place with a thin foam ring. After each field excursion, filters are returned to Huaraz where they are dried in the sun, then stored in a freezer until the end of the expedition when they are returned to the US for analysis.

3 Filter analysis

A new technique has been developed for the analyzing the light absorption properties of particles collected on filters. The Light Absorption Heating Method (LAHM) is a cost effective technique that can be used to accurately quantify the impact of light-absorbing particles on snow. The premise behind conducting measurements of light-absorbing particles in snow is to estimate the amount of light energy the particles will absorb leading to increased melting or sublimation. Because snow is completely absorptive in the thermal infrared wavelength range, the more critical wavelengths to consider are in the visible range. Understanding the absorption of solar radiation in the visible wavelength range by particles in snow is the goal of the research. The LAHM analysis technique described here approaches the problem directly by measuring the temperature increase of a particle load on a filter when visible light is applied. A diagram of the LAHM setup is shown in Fig. 1. Each filter is suspended on plastic wrap a few centimeters above a pool of cool water. Water is used because it provided a thermally stable background compared to a solid surface which could absorb visible radiation. Plastic wrap does not absorb visible light, and as such it provides a neutral background and is of low mass per unit area thus having a negligible effect on measurements. An infrared thermometer (IR thermometer: Omega OS1327D) which can record data every second is mounted above the filter to measure the temperature of the filter without touching it. To determine the light absorption ability of the materials, a laboratory grade light source (Cole-Parmer Fiber-Lite Fiber Optical Illuminator model 9745-00) with a fiber optic light pipe to direct the light is mounted close to the filter and shines light at approximately a 45° angle to the filter (thus reducing the effects of multiple reflections in the system). The light transmitted through the light pipe only spans the visible wavelengths from 300–800 nm. The particles on the filter absorb light causing the filter to warm. The IR thermometer records the temperature of the filter every second, and data are saved to a computer for later analysis. After an initial 10 s to establish a base temperature, the light source is turned on for 30 s, then extinguished while the temperature of the filter is recorded for an additional 50 s. Temperature increases are normalized by the average temperature recorded during the first 10 s. The maximum temperature increase of a filter ranges from less than 1 °C for a clean filter, up to 10 °C for the most heavily contaminated filters. During analysis, after every 10 filters, 2 control filters were tested to assure consistency in the setup. The control filters included an unused clean filter and a calibration filter with a heavy load of BC. Sample temperature profiles from seven filters collected during the 2011 expedition are shown in Fig. 2.

The LAHM analysis technique was calibrated by sampling a BC standard: water with a known concentration of BC (Schwarz et al., 2012). The BC standard has 10% uncertainty. Filters with low and high BC loads were made by

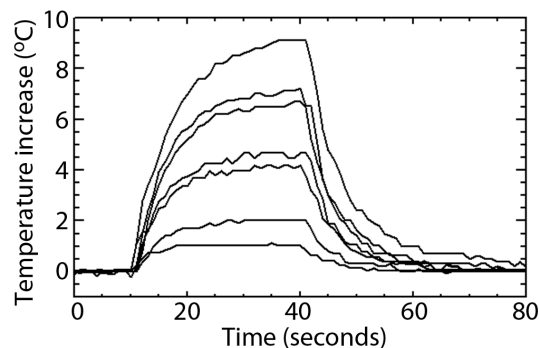


Figure 2. Measured temperature profiles for seven filters with a variety of light-absorbing particle loads. Temperature recording started 10 s before the lamp was illuminated, and the lamp was extinguished 30 s later. Temperatures are normalized to the average of first 10 s of data and the temperature usually returned to the start temperature within a minute of the lamp being extinguished.

filtering different amounts of BC standard. The BC standard was made with fullerene soot, a reference material used in the single-particle BC detection community (Baumgardner et al., 2012). The filters used for calibration (Millipore mixed cellulose ester filter membrane 0.22 micron) are different from the filters that have been used in the field (Pallflex Membrane Tissuquartz 0.7 micron). The BC standard was created with BC particles in the size range generally found in the atmosphere (0.2 to 0.8 microns) which were not captured well by the Tissuquartz filters. Torres et al. (2014) found that Tissuquartz filters captured less than 38% of the BC mass when filtering rainwater. The mass size distribution for their measurements peaked between 210 and 240 nm, similar to atmospheric BC sizes but smaller than the peak sizes expected in snow (Schwarz et al., 2012). The Tissuquartz filters are used in the field because water flow through the filters is much faster making them much easier to use in the field and the filter material enables additional types of analysis that are not possible with the Millipore filters. Temperature profiles recorded for unused filters of both types were nearly identical (well within the SD of measurements), indicating that the filter type did not bias the temperature measurement technique significantly. Three calibration filters at each of four different fullerene soot mass amounts (5–20 µg) were created as well as one calibration filter with 30.0 µg. The temperature increase for each calibration filter was determined at least 4 times, and the overall standard deviation in the temperature increase at each carbon level was used in the uncertainty determination. Figure 3 shows plots of 12 temperature increase profiles measured for the three calibration filters loaded with 10 µg of fullerene soot. The mean values and standard deviations are also shown, along with a calibration curve showing the relationship between BC mass and heating after 10 s. Standard deviation values were generally less than 0.5 °C and remained constant throughout the heating phase. Note that

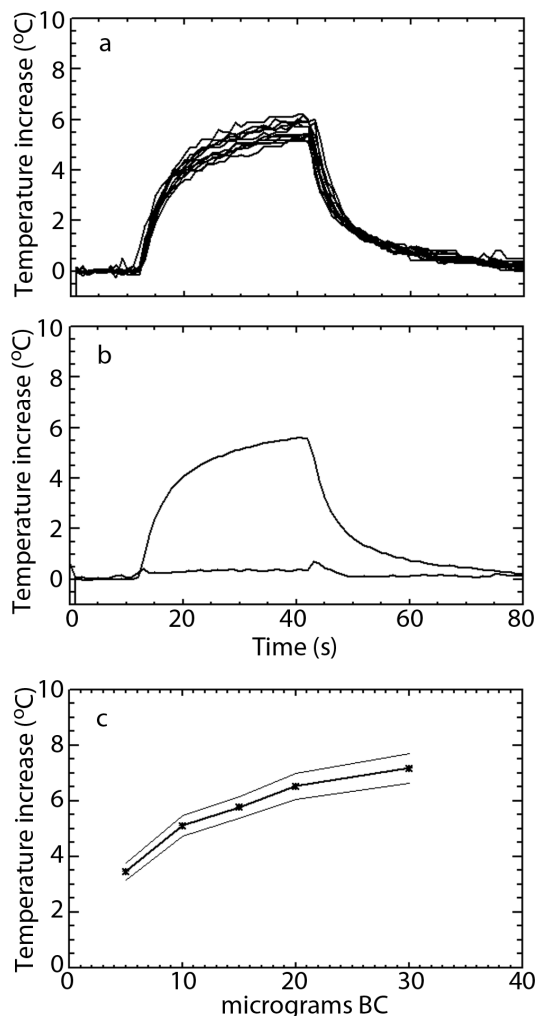


Figure 3. (a) Twelve temperature profiles measured for filters with 10 μg of fullerene soot. Profiles are from three different filters measured 4 times each. (b) Mean temperature profile and standard deviation for 12 temperature profiles shown in (a). (c) Temperature increases after 10 s for five masses of fullerene soot. Error bars are standard deviations for each measurement and bold line is fit to data.

the heating for blank filters was approximately 0.6°C on average, just above the SD for the shown measurements. Several of the cleanest filters from mountain samples from each year had temperature increases of less than 1.0°C .

Laboratory measurements of post-filtered samples showed that the Tissuquartz filters did not efficiently collect BC particles smaller than about 0.6 microns. In the atmosphere most BC mass is distributed across particles smaller than this, but BC in snow has been shown to exist, in some samples, at sizes up to a few microns (Schwarz et al., 2012). While it is clear that the Tissuquartz filters may not be collecting all of the BC, it is unclear what portion is being missed. Results of separate mineralogy tests suggest that there were high concentrations of dust which can clog the pores and anecdotal

evidence (volunteers noting that it had become very difficult to push the water through the filters) suggests that the effective pore size substantially decreases as dusty samples are being filtered. Given that BC particles in this size range can be missed, the BC on the sample filters is likely an underestimate of the true BC in the snow. Since this under-catch was noticed, tests have been conducted using snow from tropical glaciers that indicate that the missed particles do not account for much absorption. Snow sourced water that had already been passed through a Tissuquartz filter was collected and passed through a 0.22 micron filter. While the Tissuquartz filters in these tests captured high concentrations of particles, the 0.22 micron filters appeared clean after filtering and results from the LAHM technique were below the detection threshold. Of the approximately 20 tests filters, the eBC (effective black carbon) value estimated for the 0.22 micron filter was never more than 20 % of the value determined for the Tissuquartz filter and the average was around 5 %, well within the noise level of the LAHM technique at these levels.

The LAHM technique does not discriminate between BC and dust. Therefore, the values derived from the LAHM technique should be treated as eBC, meaning that the visible light absorptive capacity of the particles on the sample filter are equivalent to the given amount of BC (Grenfell et al., 2011).

The increase in temperature of the calibration filters after 10 s of exposure to light was used to derive a fit equation to predict the mass of BC on the calibration filters. The r^2 value of the fit equation was 0.98 with an uncertainty of approximately $\pm 20\%$ (10 % from the BC standard and 10 % for the typical SD calculated and shown in Fig. 3b). This uncertainty likely increases with higher filter loads given that the temperature response to BC curve flattens (Fig. 3c). On heavily loaded filters, this flattening could be due to some of the BC being hidden under other layers of particles and therefore not absorbing as much light energy as other BC on the filter. It was found, however, that filter samples collected in the field often had different slopes to their temperature increase, particularly after 20 s of illumination. It is suspected that this is due to dust mixed in with the BC changing the overall heat capacity. Figure 4 shows two temperature profiles, one from a fullerene soot calibration filter and one from a sample filter suspected to contain significant dust as well as a substantial amount of BC. Note that the temperature curves are nearly identical for approximately 10 s after illuminating the lamp before they begin to diverge. It is thought that dust mixed in with BC on a filter could be causing this divergence. Filters collected in other regions with substantially higher dust concentrations and low BC concentrations showed much steeper temperature increases later in the heating phase. This would suggest that the effects of BC and dust could be separated with the LAHM technique, but quantification of this is beyond the scope of this publication.

Data from 2011 were collected with a slightly different filtering setup than subsequent expeditions. The change was made because the type of filter housing used in 2011 occa-

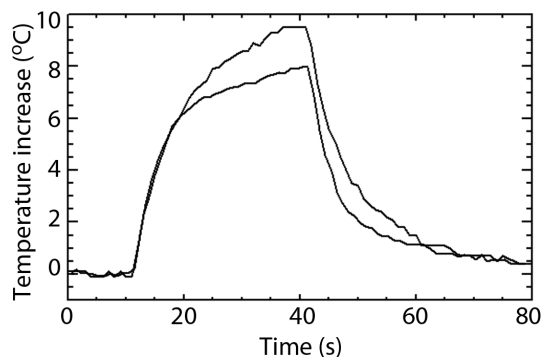


Figure 4. Temperature profiles measured for a calibration filter with fullerene soot (lower curve), and a sample filter with dust and black carbon (upper curve). The curves are nearly identical until 20 s (10 s of heating) after which they diverge. The continued more rapid increase in temperature of the dust – black carbon mixture is thought to be due to the dust.

sionally came into contact with the surface of the filter leading to the removal of some of the particles when the filter housing was opened. We estimate that this may have reduced the filter loading by up to 25%. This estimate is based on the approximate area of the filter that appeared to be scraped clean as well as the fact that the filter holder had obvious particle loading that corresponded to the cleaned area. While it is not possible to determine the exact amount of material lost, the eBC values estimated for the affected filters were multiplied by 1.25.

During the 2013 expedition, 12 unmelted snow samples were collected in acid washed glass vials and returned to the US for analysis with a Single Particle Soot Photometer (SP2) instrument (see Schwarz et al., 2012). These samples were collected from two mountains: one in a region suspected to be highly polluted due to its proximity to Huaraz and another mountain in a more remote region. Additional snow samples were collected for filtering from the same locations for comparison. Results from the LAHM technique are compared to SP2 refractory black carbon (rBC; Baumgardner et al., 2012) mass concentration measurements in Fig. 5. Note that while there is some variability between the techniques, the results are reasonably correlated ($r^2 = 0.92$). Microscale variability could have accounted for some of the differences. Figure 5 shows that for some of the comparisons, the SP2 rBC values were higher than the LAHM eBC values. This could be due to non-uniformity in snow as the LAHM technique uses much more snow than the SP2 (600 g for LAHM vs. ~ 10 g for SP2). Additionally, the Tissuquartz filter could have missed a fair amount of the BC mass due to the large pore size.

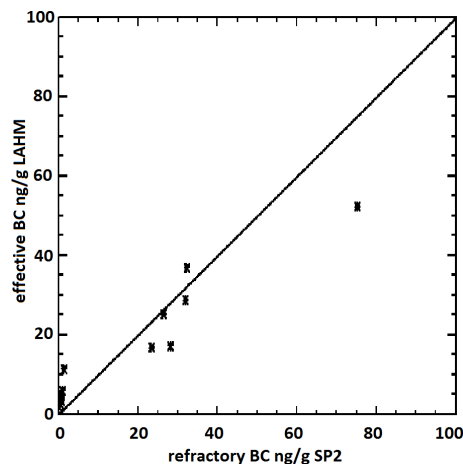


Figure 5. Plot showing the relationship between eBC as determined from the LAHM analysis and refractory black carbon as determined by the SP2 instrument ($r^2 = 0.92$). The values near 0.0 refractory BC are from Pisco mountain in region 2 while the higher values are from Vallunaraju in region 4. The 1 to 1 line is plotted to guide the eye.

4 Results

The eBC values determined by the LAHM technique for all measurements collected during the three expeditions are shown in Fig. 6 plotted by altitude. Values of eBC range from the quite low: $2.0 \text{ ng-eBC g-H}_2\text{O}^{-1}$ up to almost 80 ng g^{-1} . The highest altitudes have substantially less eBC while lower altitude values were larger; although numerous measurements still show values of less than 10.0 ng g^{-1} eBC at low altitudes. The largest values are similar to those reported by Ye et al. (2012) who reported values between 20 and 70 ng g^{-1} of BC in northwestern China seasonal snow at altitudes up to 3500 m. Huang et al. (2011) measured much larger values (over 1000 ng g^{-1}) of eBC in northeastern China, where dust was common as well as high levels of BC. The Cordillera Blanca measurements of eBC compare similarly in value and variability to those observed by Doherty et al. (2013) in Alaska and Greenland and are similar to those reported by Grenfell et al. (1981) for the Washington Cascade mountains ($22\text{--}59 \text{ ng g}^{-1}$). The values are somewhat lower than those reported by Sargent et al. (1993) for the French Alps ($80\text{--}280 \text{ ng g}^{-1}$).

4.1 Surface accumulation

As stated in the field measurements section, it was rare to collect samples where the surface sample contained long term dry deposition and surface accumulation and the subsurface sample contained only pristine snow. Often, the snow from the previous storm had compacted enough that the subsurface sample contained snow that had been previously exposed as a surface. This led to the eBC values for the surface and sub-

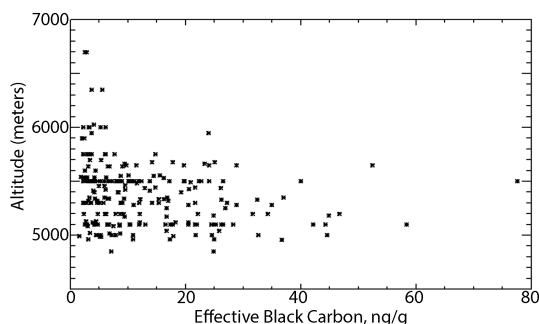


Figure 6. complete data set of eBC values determined from the LAHM analysis plotted versus altitude.

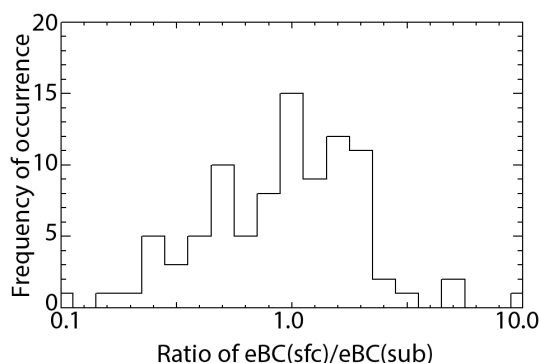


Figure 7. Probability distribution function of the ratio of the eBC value measured for surface samples divided by the eBC value measured for subsurface samples presented. x axis is on a log scale and bins are logarithmically spaced.

surface samples to not be consistently related. During the 3 expeditions there were 92 paired measurements where a surface sample and a subsurface sample were collected. Of those samples, in 56 cases, the surface sample contained higher eBC values than the subsurface samples while for the remaining 36 samples the opposite was true. The average ratio (averaged in log-space) was 0.96 suggesting that on the average, the surface and subsurface samples were statistically similar. The average difference between the two samples was a factor of 2.17 with a maximum difference of a factor of 12. Based on the fact that it does snow from time to time in the dry season, and that samples are never collected near the zone of ablation, the differences are thought to be due to short term changes in the snow pack rather than annual variability. Figure 7 shows a probability distribution function of the ratio between the surface measurement to the subsurface measurement for the 92 pairs of measurements.

4.2 By region

Figure 8 shows a map of the Cordillera Blanca region and the eBC values in snow determined from filter samples using the LAHM analysis technique for filter samples collected in

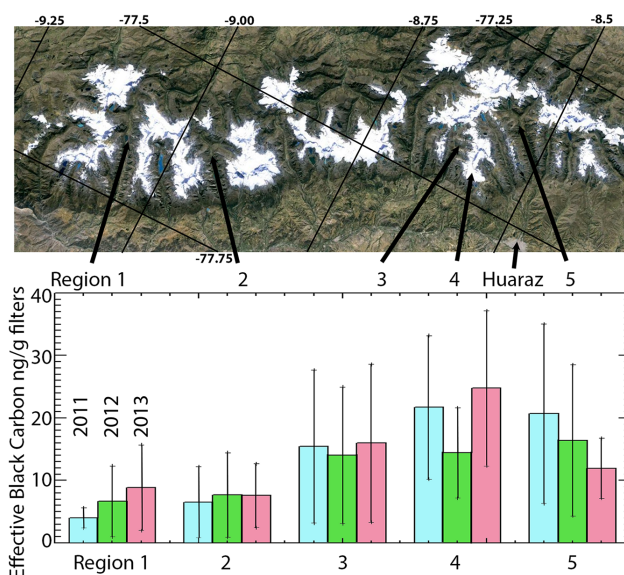


Figure 8. Google map image of the Cordillera Blanca mountain range. The five regions as well as the city of Huaraz are indicated on the map by black arrows. Average eBC values as determined from the LAHM analysis are shown in the plot for each of the 3 years. The thin lines indicate ± 1 standard deviation of the measurements. Note that in 2013, region 2, SP2 samples averaged 0.65 ng g^{-1} rBC indicating that most of the 8 ng g^{-1} of the eBC estimate could be due to light absorption by dust.

different areas during each of the three expeditions. For the three expeditions, the data are grouped into five different valleys or mountains that were sampled each of the 3 years. Regions 1 and 2 lie on the north end of the range and consist of the mountains in the Santa Cruz and Paron valleys (region 1, 70 km from Huaraz), and Llanganuco valley (region 2, 54 km from Huaraz). These regions are characterized by higher precipitation and lower nearby population densities. The mountains around Ishinca valley (region 3, 21 km from Huaraz), Vallunaraju mountain (region 4, 14 km from Huaraz), and the mountains around the Quilcayhuanca valley (region 5, 24 km from Huaraz) are all clustered near Huaraz, the largest population center in the region. The eBC values shown in Fig. 8 are determined by taking an average of all measurements of surface and subsurface snow in each of the regions. As the relationship between the surface and subsurface values was highly variable (as shown in Fig. 7), the averaged values are thought to better represent the typical conditions for the top 10 cm of snow. Standard deviations of the measurements in each region are shown in Fig. 8. Data from all 3 years show a distinct trend, with the southern regions having 2–3 times more light-absorbing particles compared to the northern regions. The SP2 measurements discussed in the calibration section were collected in 2013 in region 2 and 4. The region 2 SP2 measurements averaged 0.65 ng g^{-1} while the region 4 SP2 values averaged 31.0 ng g^{-1} . The LAHM technique suggests that the eBC values in region 1 and 2 would be on the

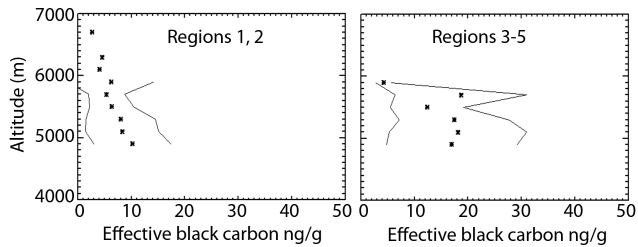


Figure 9. LAHM determined eBC values averaged by altitude bins plotted with ± 1 standard deviation (lines) by altitude for the northern (regions 1 and 2) mountains and the southern (regions 3–5) mountains in the Cordillera Blanca. Absorbing particles in snow in regions 1 and 2 are likely primarily dust while regions 3–5 are strongly influenced by pollution from the city of Huaraz.

order of 10 ng g^{-1} while the SP2 rBC was much lower. This leads us to the hypothesis that the bulk of the temperature increase on the filters from region 1 and 2 is likely due almost exclusively to dust rather than BC, while in regions 3–5, near the city of Huaraz, BC likely makes up a substantial portion of the absorptive particle matter present on the filters because the eBC values and the SP2 rBC values are similar in magnitude in region 4. Differences observed from year to year in each region are likely due to sampling being weighted to different altitudes or mountains rather than substantial changes in pollutant levels.

Figure 9 shows the mean value and standard deviation for data collected from all 3 years separated by altitude. Data are binned into two groups: region 1 and 2 in one group and 3–5 in the second group for all 3 years combined. Note the relatively linear decrease in eBC with altitude for both regions. Thin lines show the standard deviation calculated for the more numerous measurements. In general, eBC concentration levels decrease with altitude, though it should be noted that there are few measurements at altitudes above 6000 m and those are mostly in region 2.

4.3 By depth

During the 2012 expedition, samples were collected from the wall of a newly opened crevasse on Vallunaraju mountain in region 4. Vallunaraju is the nearest glaciated mountain to Huaraz and has some of the highest eBC measurements using the LAHM technique as well as the highest concentration observed by the SP2 ($75 \text{ ng-rBC g-H}_2\text{O}^{-1}$). Figure 10 shows the eBC values for the samples collected from the crevasse wall as a function of depth in the crevasse. There were several dark streaks at relatively uniform spacing down the crevasse wall which are suspected to be surface accumulations during the dry seasons (local glaciology experts agreed with this assessment). The eBC measurements higher than 20 ng g^{-1} in Fig. 10 were from the darker areas while the lower values were from cleaner ice that dominated the crevasse wall. It is suspected that the cleaner samples were from wet season

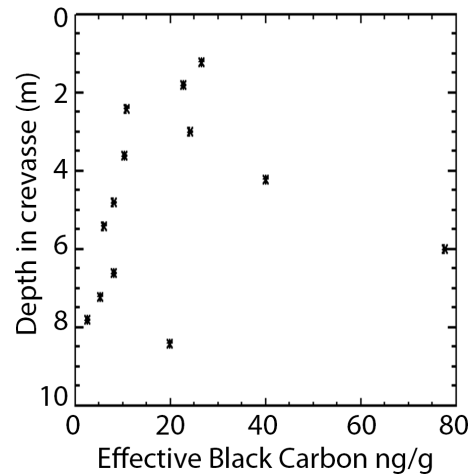


Figure 10. eBC from snow samples collected from the walls of a crevasse on Vallunaraju (region 4) the nearest high mountain to Huaraz. A decreasing trend with depth is noted. These lowest samples were visually the cleanest snow samples from the crevasse walls, and were likely to have accumulated during the wet season. The points at 4, 6, and 8.5 m were thin noticeably dark layers.

storms. A distinct decrease of eBC values with depth can be seen in the suspected wet season samples. While this might indicate that black carbon values have been increasing in recent wet seasons, the values are low enough that the trend is within the expected uncertainty range.

5 Conclusions

It is well documented that tropical glaciers are melting rapidly with concurrent effects on critical water supplies. Numerous factors could be contributing to low latitude glacier mass loss, including larger concentrations of light-absorbing particles on glacier surfaces. Because melting glacial water is an important natural resource in the region for agriculture, hydroelectric power, and drinking water, an increased understanding of the pressures on this resource could aid regional planners in adapting to future regional climate changes. This paper presents the results of 3 years of measurements of light-absorbing particles on the glaciers in the Cordillera Blanca in Peru. Samples were collected by volunteers participating in American Climber Science Program expeditions. Snow samples collected from glacier surfaces were melted, and the light-absorbing particles collected on filters.

A new technique (called the LAHM technique herein) to quantify the amount of visible radiation the light-absorbing particles can absorb has been developed and calibrated using filters with a known amount of black carbon. These “effective black carbon” estimates from the LAHM technique were found to be well correlated ($r^2 = 0.92$) with refractory black carbon mass measurements made with the Single Particle Soot Photometer instrument for a subset of the measure-

ments. The LAHM technique provides an accurate, useful, and cost effective way to measuring light-absorbing particles in snow.

In the Cordillera Blanca, the concentration of light-absorbing particles was highest near Huaraz, the largest city in the region, while samples from more remote regions contained substantially lower amounts of absorptive material. The measured levels of light-absorbing particles in the snow near Huaraz absorb a similar amount of visible radiation as snow that contains between 20 to 80 ng g⁻¹ of black carbon. This amount of black carbon in pristine fresh snow can result in a decrease in spectral albedo of greater than 1 % (SNICAR-online: Snow, Ice, and Aerosol Radiation model, Flanner et al., 2007).

Acknowledgements. This work would not have been possible without the help of the American Climber Science Program volunteers for the 2011, 2012, and 2013 expeditions. The authors specifically wish to thank Frank Nederhand for initiating the program that would lead to the ACSP and Chris Benway at La Cima Logistics in Huaraz, Peru for helping to organize the expeditions. Thanks to Darrel Baumgardner for helping to facilitate the SP2 measurements as well as for helping to bring this work to the attention of the Pollution and its Impacts on the South American Cryosphere (PISAC) Initiative. Thanks to Karl Froyd and Jin Liao for their helpful comments and analysis with the PALMS instrument. Thanks also to Huascar National Park, Jesus Gomez park director, for helping ensure the long term success of this research. Additional thanks go to the many generous donors who have made the ACSP expeditions possible. Also, the American Alpine Club whose early assistance was invaluable.

Edited by: A. Klein

References

- Baraer, M., Mark, B. G., McKenzie, J. M., Condom, T., Bury, J., Huh, K.-I., Portocarrero, C., and Gomez, J.: Glacier recession and water resources in Peru's Cordillera Blanca, *J. Glaciol.*, 58, 134–150, doi:10.3189/2012JoG11J186, 2012.
- Barnett, T. P., Adams, J. C., and Lettenmaier, D. P.: Potential impacts of a warming climate on water availability in snow-dominated regions, *Nature*, 438, 303–309, doi:10.1038/nature04141, 2005.
- Baumgardner, D., Popovicheva, O., Allan, J., Bernardoni, V., Cao, J., Cavalli, F., Cozic, J., Diapouli, E., Eleftheriadis, K., Genberg, P. J., Gonzalez, C., Gysel, M., John, A., Kirchstetter, T. W., Kuhlbusch, T. A. J., Laborde, M., Lack, D., Müller, T., Niessner, R., Petzold, A., Piazzalunga, A., Putaud, J. P., Schwarz, J., Sheridan, P., Subramanian, R., Swietlicki, E., Valli, G., Vecchi, R., and Viana, M.: Soot reference materials for instrument calibration and intercomparisons: a workshop summary with recommendations, *Atmos. Meas. Tech.*, 5, 1869–1887, doi:10.5194/amt-5-1869-2012, 2012.
- Bradley, R. S., Vuille, M., Diaz, H. F., and Vergara, W.: Threats to water supplies in the tropical Andes, *Science*, 312, 1755–1756, doi:10.1126/science.1128087, 2006.
- Bradley, R. S., Keimig, F. T., Dias, H. F., and Hardy, R. D.: Recent changes in freezing level heights in the tropics with implications for the deglaciation of high mountain regions, *Geophys. Res. Lett.*, 36, L17701, doi:10.1029/2009GL037712, 2009.
- Doherty, S. J., Warren, S. G., Grenfell, T. C., Clarke, A. D., and Brandt, R. E.: Light-absorbing impurities in Arctic snow, *Atmos. Chem. Phys.*, 10, 11647–11680, doi:10.5194/acp-10-11647-2010, 2010.
- Doherty, S. J., Grenfell, T. C., Forsström, S., Hegg, D. L., Brandt, R. E., and Warren, S. G.: Observed vertical redistribution of black carbon and other insoluble light-absorbing particles in melting snow, *J. Geophys. Res.-Atmos.*, 118, 5553–5569, doi:10.1002/jgrd.50235, 2013.
- Flanner, M. G., Zender, C. S., Randerson, J. T., and Rasch, P. J.: Present day climate forcing and response from black carbon in snow, *J. Geophys. Res.*, 112, D11202, doi:10.1029/2006JD008003, 2007.
- Grenfell, T. C., Perovich, D. K., and Ogren, J. A.: Spectral albedos of an alpine snowpack, *Cold Reg. Sci. Technol.*, 4, 121–127, 1981.
- Grenfell, T. C., Doherty, S. J., Clarke, A. D., and Warren, S. G.: Light absorption from particulate impurities in snow and ice determined by spectrophotometric analysis of filters, *Appl. Optics*, 50, 1–12, 2011.
- Huang, J., Fu, Q., Zhang, W., Wang, X., Zhang, R., Ye, H., and Warren, S. G.: Dust and black carbon in seasonal snow across northern China, *B. Am. Meteorol. Soc.*, 92, 175–181, doi:10.1175/2010BAMS3064.1, 2011.
- Kaiser, J. W., Heil, A., Andreae, M. O., Benedetti, A., Chubarova, N., Jones, L., Morcrette, J.-J., Razinger, M., Schultz, M. G., Suttie, M., and van der Werf, G. R.: Biomass burning emissions estimated with a global fire assimilation system based on observed fire radiative power, *Biogeosciences*, 9, 527–554, doi:10.5194/bg-9-527-2012, 2012.
- Kalnay, E., Kanamitsu, M., Kistler, R., Collins, W., Deaven, D., Gandin, L., Iredell, M., Saha, S., White, G., Woollen, J., Zhu, Y., Chelliah, M., Ebisuzaki, W., Higgins, W., Janowiak, J., Mo, K. C., Ropelewski, C., Wang, J., Leetmaa, A., Reynolds, R., Jenne, R., and Joseph, D.: The NCEP/NCAR 40-year reanalysis project, *B. Am. Meteorol. Soc.*, 77, 437–471, 1996.
- Kaser, G.: A review of the modern fluctuations of tropical glaciers, *Global Planet Change*, 22, 93–103, 1999.
- Lamarque, J.-F., Bond, T. C., Eyring, V., Granier, C., Heil, A., Klimont, Z., Lee, D., Lioussé, C., Mieville, A., Owen, B., Schultz, M. G., Shindell, D., Smith, S. J., Stehfest, E., Van Aardenne, J., Cooper, O. R., Kainuma, M., Mahowald, N., McConnell, J. R., Naik, V., Riahi, K., and van Vuuren, D. P.: Historical (1850–2000) gridded anthropogenic and biomass burning emissions of reactive gases and aerosols: methodology and application, *Atmos. Chem. Phys.*, 10, 7017–7039, doi:10.5194/acp-10-7017-2010, 2010.
- Mark, B. G. and Seltzer, G. O.: Tropical glacier meltwater contribution to stream discharge: a case study in the Cordillera Blanca, Peru, *J. Glaciol.*, 49, 271–281, 2003.
- Painter, T. H., Deems, J. S., Belnap, J., Hamlet, A. F., Landry, C. C., and Udall, B.: Response of Colorado river runoff to dust ra-

- diative forcing in snow, *P. Natl. Acad. Sci.*, 107, 17125–17230, doi:10.1073/pnas.0913139107, 2010.
- Painter, T. H., Skiles, S. M., Deems, J. S., Bryant, A. C., and Landry, C. C.: Dust radiative forcing in snow of the upper Colorado river basin: 1. A 6 year record of energy balance, radiation, and dust concentrations, *Water Resour. Res.*, 48, W07521, doi:10.1029/2012WR011985, 2012.
- Painter, T. H., Flanner, M. G., Kaser, G., Marzeion, B., VanCuren, R. A., and Abdalati, W.: End of the Little Ice Age in the Alps forced by industrial black carbon, *P. Natl. Acad. Sci.*, 110, 15216–15221, doi:10.1073/pnas.1302570110, 2013.
- Rabatel, A., Francou, B., Soruco, A., Gomez, J., Cáceres, B., Ceballos, J. L., Basantes, R., Vuille, M., Sicart, J.-E., Huggel, C., Scheel, M., Lejeune, Y., Arnaud, Y., Collet, M., Condom, T., Consoli, G., Favier, V., Jomelli, V., Galarraga, R., Ginot, P., Maisincho, L., Mendoza, J., Ménégoz, M., Ramirez, E., Ribstein, P., Suarez, W., Villacis, M., and Wagnon, P.: Current state of glaciers in the tropical Andes: a multi-century perspective on glacier evolution and climate change, *The Cryosphere*, 7, 81–102, doi:10.5194/tc-7-81-2013, 2013.
- Schauwecker, S., Röhrer, M., Acuna, D., Cochichin, A., Davila, L., Frey, H., Giraldez, C., Gomez, J., Huggel, C., Jacques-Coper, M., Loarte, E., Salzmann, N., and Vuille, M.: Climate trends and glacier retreat in the cordillera blanca, Peru, revisited, *Global Planet. Change*, 119, 85–97, 2014.
- Schwarz, J. P., Doherty, S. J., Li, F., Ruggiero, S. T., Tanner, C. E., Perring, A. E., Gao, R. S., and Fahey, D. W.: Assessing Single Particle Soot Photometer and Integrating Sphere/Integrating Sandwich Spectrophotometer measurement techniques for quantifying black carbon concentration in snow, *Atmos. Meas. Tech.*, 5, 2581–2592, doi:10.5194/amt-5-2581-2012, 2012.
- Sergent, C., Pougatch, E., and Sudul, M.: Experimental investigation of optical snow properties, *Ann. Glaciol.*, 17, 281–287, 1993.
- Torres, A., Bond, T. C., Lehmann, C. M. B., Subramanian, R., and Hadley, O. L.: Measuring organic carbon and black carbon in rainwater: evaluation of methods, *Aerosol Sci. Tech.*, 48, 239–250, doi:10.1080/02786826.2013.868596, 2014.
- Vuille, M., Francou, B., Wagnon, P., Juen, I., Kaser, G., Mark, B. G., and Bradley, R. S.: Climate change and tropical Andean glaciers: past, present and future, *Earth-Sci. Rev.*, 89, 79–96, doi:10.1016/j.earscirev.2008.04.002, 2008.
- Warren, S. G. and Wiscombe W. J.: A model for the spectral albedo of snow II: Snow containing atmospheric Aerosols, *J. Atmos. Sci.*, 37, 2734–2745, 1980.
- Ye, H., Zhang, R., Shi, J., Huang, J., Warren, S. G., and Fu, Q.: Black carbon in seasonal snow across northern Xinjiang in north-western China, *Environ. Res. Lett.*, 7, 1–9, doi:10.1088/1748-9326/7/4/044002, 2012.